Electronic Supplementary Material (ESI) for Journal of Materials Chemistry C.


*Supporting information*

# Strategic carbazole-cycloalkyl fused donors to induce TADF featured AIE for high efficiency deep blue emission

**Jae Hee Lee,‡[a] Yeonju Jeong,‡[b] Jairam Tagare,[a] Min Jeong Kwon,[a] Taekyung Kim*[bc] and Wan Pyo Hong*[a]**

[a]Department of Chemistry, Gachon University, Seongnam-si, Gyeonggi-do, 13120, Korea

[b]Department of Information Display, Hongik University, Seoul, 04066, Korea

[c]Department of Materials Science and Engineering, Hongik University, Sejong, 30016, Korea

## I. Supplementary Schemes, Figures and Tables

## I. Supplementary Figures, Scheme and Tables

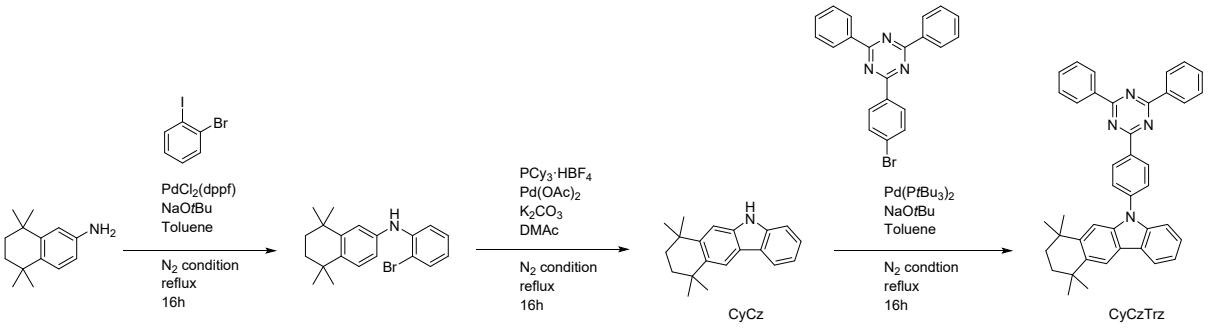


**Scheme S1**. Synthetic route of CyCzTrz

*Synthesis of* 5-(4-(4,6-diphenyl-1,3,5-triazin-2-yl)phenyl)-7,7,10,10-tetramethyl-7,8,9,10-tetrahydro-5H-benzo[b]carbazole (**CyCzTrz)**:

5,5,8,8-tetramethyl-5,6,7,8-tetrahydronaphthalen-2-amine (5.00 g, 24.6 mmol) and 1-bromo-2-iodobenzene (7.30 g, 25.9 mmol) were dissolved in 100 ml of toluene containing sodium *tert*-butoxide (NaO*t*Bu) (3.31 g, 34.4 mmol) and 1.0 mol% of [1,1′-Bis(diphenylphosphino)ferrocene]dichloropalladium [($PdCl_2$(dppf)] as a catalyst. Under a nitrogen atmosphere, the reaction mixture was refluxed for 16 h. After cooling, the reaction mixture was extracted with ethyl acetate three times. The organic layer was separated and the moisture was removed by anhydrous $Na_2SO_4$. The solvent was removed under reduced pressure and then the crude product was purified by column chromatography on silica gel using ethyl acetate/hexane (1:20) as eluent to obtain a white powder. Yield 80.9%

The corresponding product (7.13 g, 19.9 mmol) and potassium carbonate ($K_2CO_3$) (5.50 g, 39.8 mmol) were dissolved in dimethyl acetamide (DMAc) followed by tricyclohexyl phosphine tetrafluoroborate (0.21 g, 3.98 mmol) and palladium (II) acetate was added and refluxed for 16 h under $N_2$ atmosphere. The reaction mixture was cooled and extracted with ethyl acetate three times. The organic layer was separated and the moisture was removed by anhydrous $Na_2SO_4$. The solvent was evaporated under reduced pressure and further purified by column chromatography on silica gel using ethyl acetate/hexane (1:20) to obtain a white powder: 7,7,10,10-tetramethyl-7,8,9,10-tetrahydro-5*H*-benzo[*b*]carbazole **CyCz** (4.02 g, 14.5 mmol).

Yield 72.9% $^1$H NMR (700 MHz, $CDCl_3$) δ 8.02 (dt, J=7.8, 1.0 Hz, 1H), 8.00 (s, 1H), 7.81 (s, 1H), 7.36 (s, 2H), 7.18 (ddd, J=8.0, 5.8, 2.4 Hz, 1H), 1.77 (s, 4H), 1.41 (s, 6H), 1.38 (s, 6H). $^{13}$C NMR (175 MHz, $CDCl_3$) δ 140.20, 138.26, 136.85, 125.40, 121.81, 120.06, 119.08,

117.74, 110.30, 107.70, 77.42, 35.47, 35.37, 35.00, 32.84. MS (ESI) m/z: found 278.1909. Calculated for C20H24N: 278.1909.

**CyCz** (4.02 g, 14.5 mmol) and 2-(4-bromophenyl)-4,6-diphenyl-1,3,5-triazine (5.96 g, 15.2 mmol) were dissolved in 80 ml of toluene containing sodium *tert*-butoxide (NaO*t*Bu) (2.23 g, 23.2 mmol) and 1.0 mol% of bis(tri-*tert*-butylphosphine)palladium(0) (Pd(P*t*Bu$_3$)$_2$) as a catalyst. Under a nitrogen atmosphere, the reaction mixture was stirred at a reflux for 16 h. After cooling, the reaction mixture was extracted with ethyl acetate and washed with water. The organic layer was dried over anhydrous $Na_2SO_4$, and filtered through a short silica plug. The solvent was evaporated under reduced pressure and the desired product was further purified by column chromatography. The resulting product was obtained as a white powder (6.02 g, 10.3 mmol).

Yield 71.0%, $^1$H NMR (500 MHz, $CDCl_3$) δ 9.08 – 9.02 (m, 2H), 8.88 – 8.82 (m, 4H), 8.14 (d, *J* = 7.4 Hz, 1H), 8.12 (s, 1H), 7.85 – 7.81 (m, 2H), 7.68 – 7.60 (m, 2H), 7.55 (d, *J* = 9.5 Hz, 1H), 7.42 (ddd, *J* = 8.3, 7.2, 1.2 Hz, 1H), 7.32 – 7.28 (m, 1H), 1.81 (s, 4 H), 1.48 (s, 6H), 1.38 (s, 6H). $^{13}$C NMR (125 MHz, $CDCl_3$) δ 171.80, 171.01, 144.28, 142.09, 140.89, 139.02, 137.99, 136.18, 134.47, 132.65, 130.65, 129.03, 128.70, 126.41, 125.78, 123.89, 122.16, 120.17, 117.91, 109.87, 106.99, 35.39, 35.37, 35.18, 34.58, 32.80, 32.60. MS (ESI) m/z: found 585.3015. Calculated for C41H37N4: 585.3018.

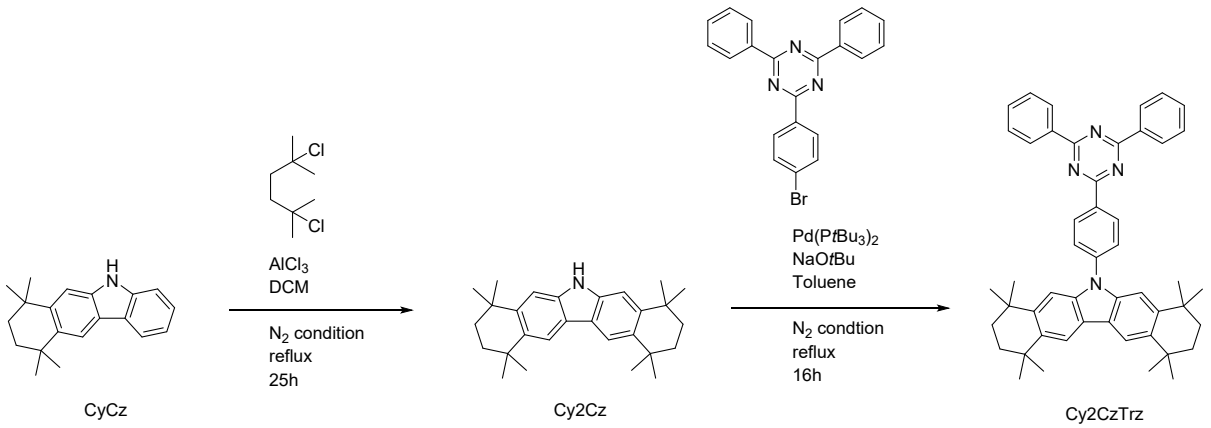

**Scheme S2**. Synthetic route of Cy2CzTrz

*Synthesis of* 6-(4-(4,6-diphenyl-1,3,5-triazin-2-yl)phenyl)-1,1,4,4,8,8,11,11-octamethyl-2,3,4,6,8,9,10,11-octahydro-1H-dibenzo[b,h]carbazole (**Cy2CzTrz)**:

To a stirring solution of 2,5-dichloro-2,5-dimethylhexane **(**3.63 g, 19.8 mmol) and **CyCz** (5.0 g, 18.0 mmol) in dried dichloromethane (100 mL), $AlCl_3$ (0.78 g, 5.40 mmol) was added in three portions over 15 min. After stirring for an additional 0.5 h, the reaction mixture was refluxed for 24 h. After cooling, the reaction mixture was extracted with ethyl acetate three times. The organic layer was separated and the moisture was removed by anhydrous $Na_2SO_4$. The solvent was removed under reduced pressure and then the crude product was purified by column chromatography on silica gel using hexane as eluent to obtain Cy2Cz a white powder.

Yield 62.8%, $^1$H NMR (700 MHz, $CDCl_3$) δ 8.16 (s, 4H), 1.84 (s, 8H), 1.47 (s, 24H). $^{13}$C NMR (175 MHz, $CDCl_3$) δ 150.13, 142.17, 125.76, 77.43, 35.28, 34.66, 32. 53. MS (ESI) m/z: found 401.2958. Calculated for C28H37N2: 401.2957.

The corresponding product (4.39 g, 11.3 mmol) and 2-(4-bromophenyl)-4,6-diphenyl-1,3,5-triazine (4.64 g, 11.8 mmol) were dissolved in 80 ml of toluene containing 1.6 eq sodium tert-butoxide and 1.0 mol% of $Pd(P\textit{t}Bu_3)_2$ as a catalyst. Under a nitrogen atmosphere, the reaction mixture was stirred at a reflux for 16 h. After cooling, the reaction mixture was extracted with ethyl acetate and washed with water. The organic layer was dried over anhydrous $Na_2SO_4$, and filtered through a short silica plug. The solvent was evaporated under reduced pressure and the desired product was further purified by column chromatography. The resulting product was obtained as a white powder (5.33 g, 7.68 mmol).

Yield 68.0%, $^1$H NMR (500 MHz, $CDCl_3$) δ 9.03 (m, 2H), 8.83 (m, 4H), 8.02 (s, 2H), 7.83 (m, 2H), 7.64 (m, 6H), 7.50 (s, 2H), 1.90 (s, 8H), 1.48 (s, 12H), 1.38 (s, 12H). $^{13}$C NMR (125 MHz, $CDCl_3$) δ 171.77, 171.08, 143.59, 142.65, 139.39, 137.60, 136.21, 133.82, 132.61, 130.60, 129.02, 128.69, 126.00, 122.28, 117.58, 106.73, 35.47, 35.42, 35.10, 34.54, 32.77, 32.58. MS (ESI) m/z: found 695.4114. Calculated for C49H51N4: 695.4114.

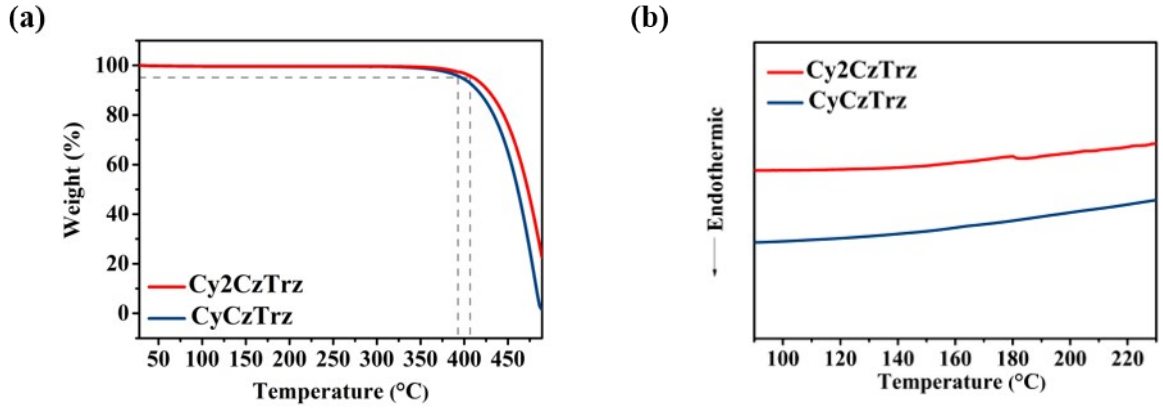


**Figure S1**. (a) TGA and (b) DSC thermograms of CyCzTrz and Cy2CzTrz recorded under nitrogen at a heating rate of $10℃$/min.

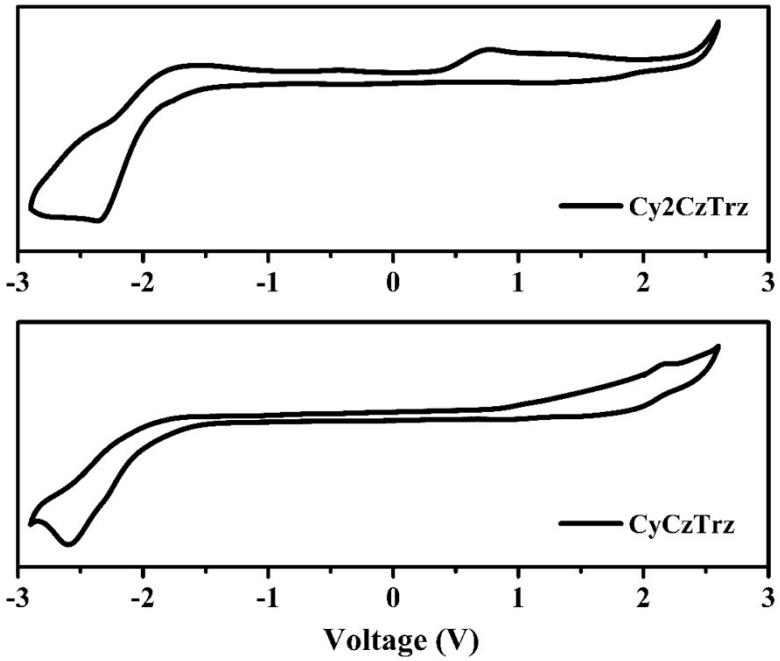


**Figure S2**. The cyclic voltammograms of CyCzTrz and Cy2CzTrz in $CH_2Cl_2$ solution containing 0.1 M TBAP electrolytes, scanning rate: 0.1 V/s.

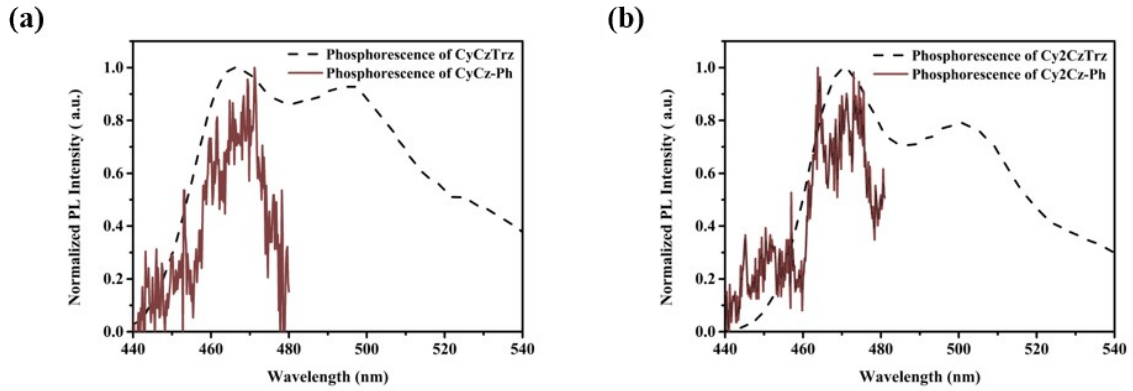


**Figure S3**. LTPH spectra of (a) CyCzTrz, (b) Cy2CzTrz and their carbazole-phenyl fragments in frozen 2-MeTHF at 77 K.

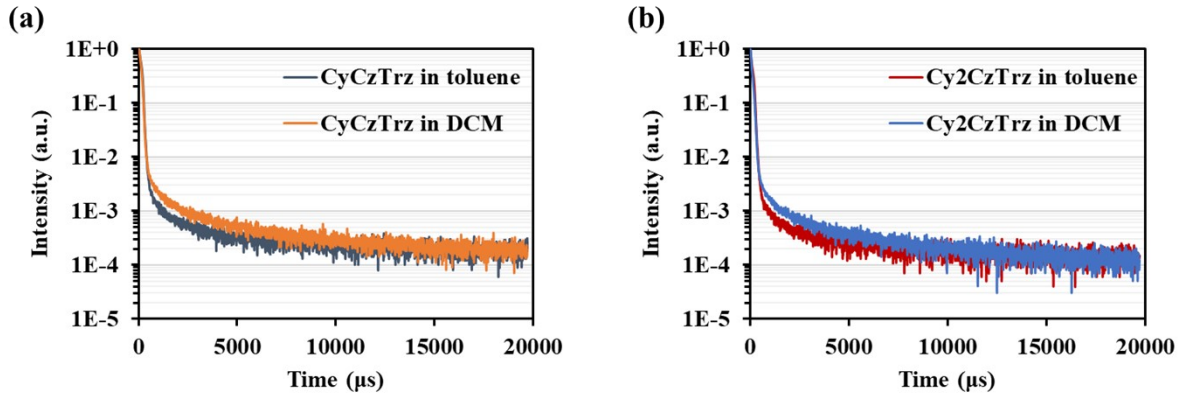


**Figure S4**. The transient photoluminescence (PL) decay of the (a) CyCzTrz and (b) Cy2CzTrz in toluene and DCM at a concentration of $2\times10^{-5}$ M.

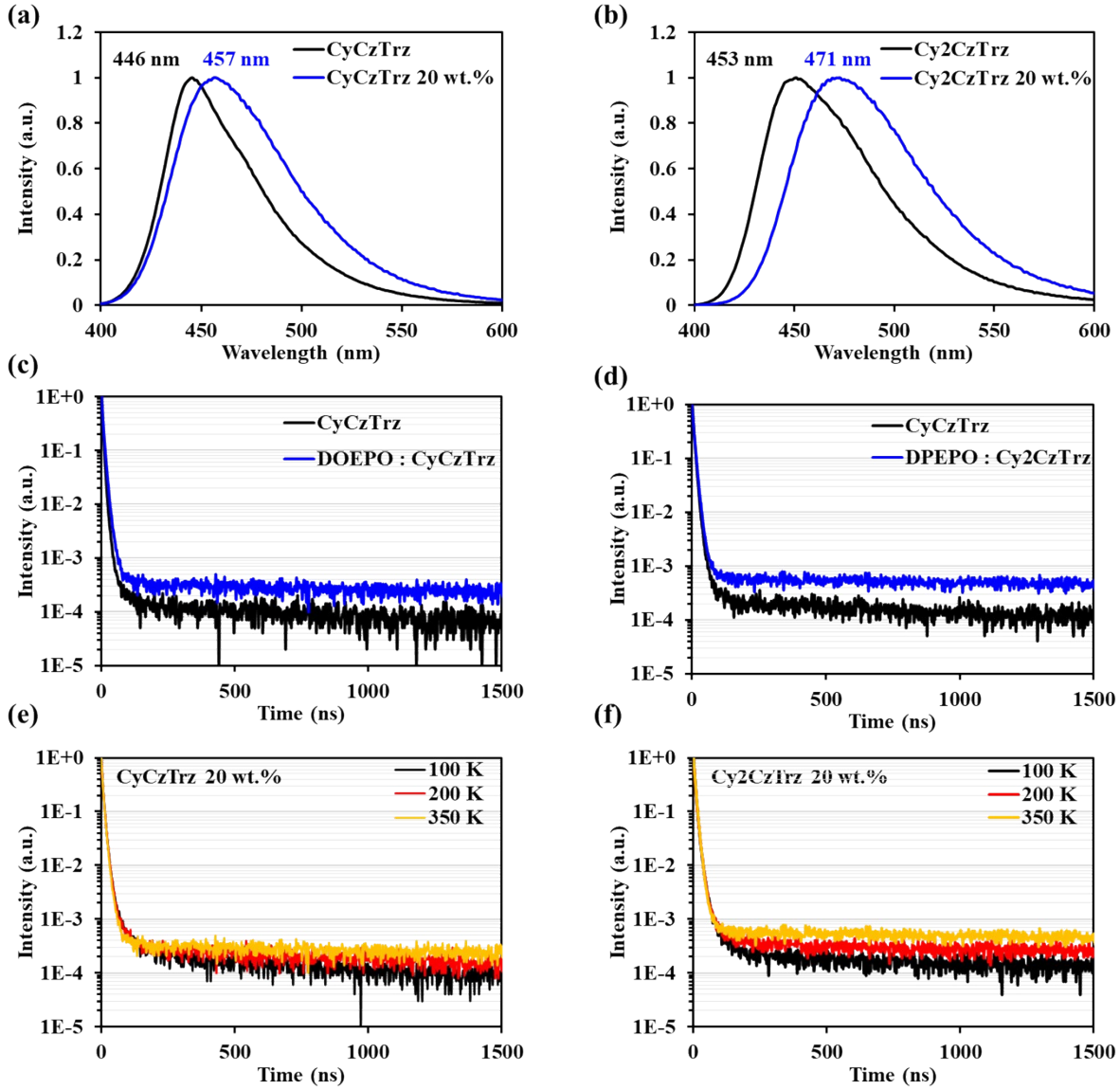


**Figure S5**. The PL spectra of (a) CyCzTrz neat film and Cy2CzTrz doped film and (b) Cy2CzTrz neat film and Cy2CzTrz doped film at room temperature. The transient PL decay of (c) CyCzTrz neat film and doped film, and (d) Cy2CzTrz neat film and doped film at room temperature. The temperature-dependent transient PL decay of (e) CyCzTrz doped film and (f) Cy2CzTrz doped film.

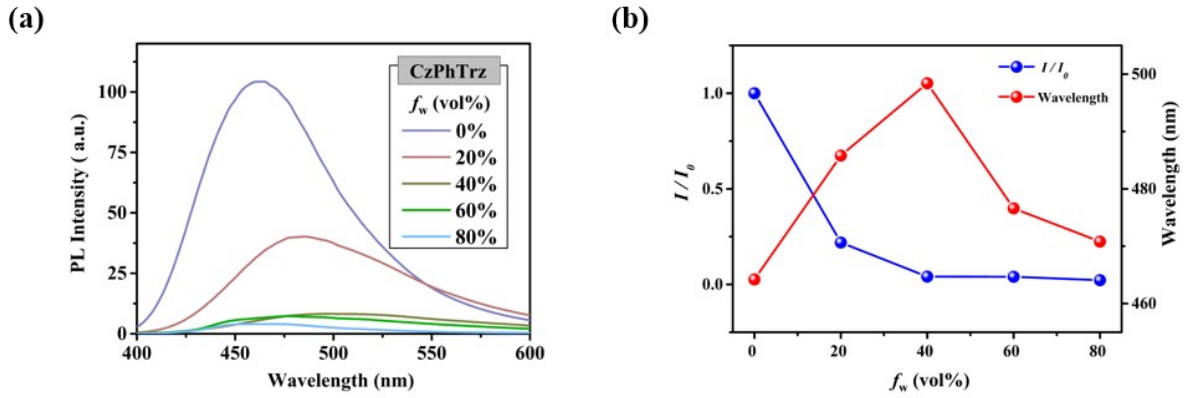


**Figure S6**. PL spectra acquired from THF-water mixtures (10 μM) with different water fractions (fw) (left) and corresponding emission intensity-peak wavelength-water volume fraction data of CzPhTrz.

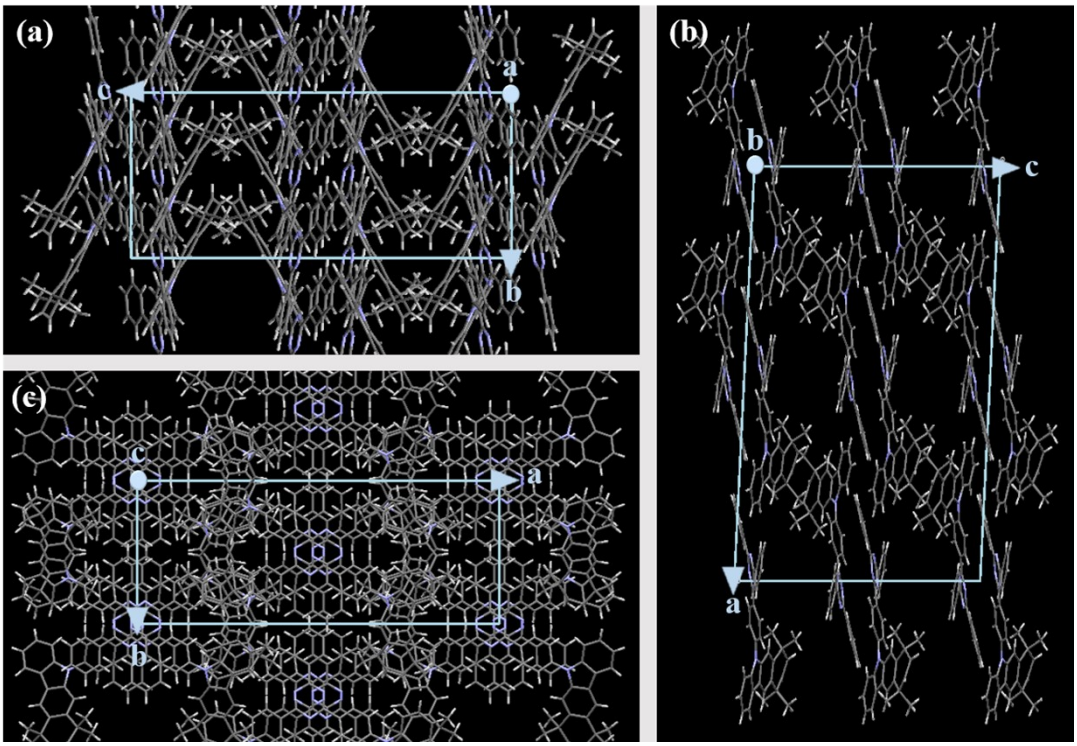


**Figure S7**. Views of molecular packing of CyCzTrz from (a) *a* axis, (b) *b* axis and (C) *c* axis, respectively.

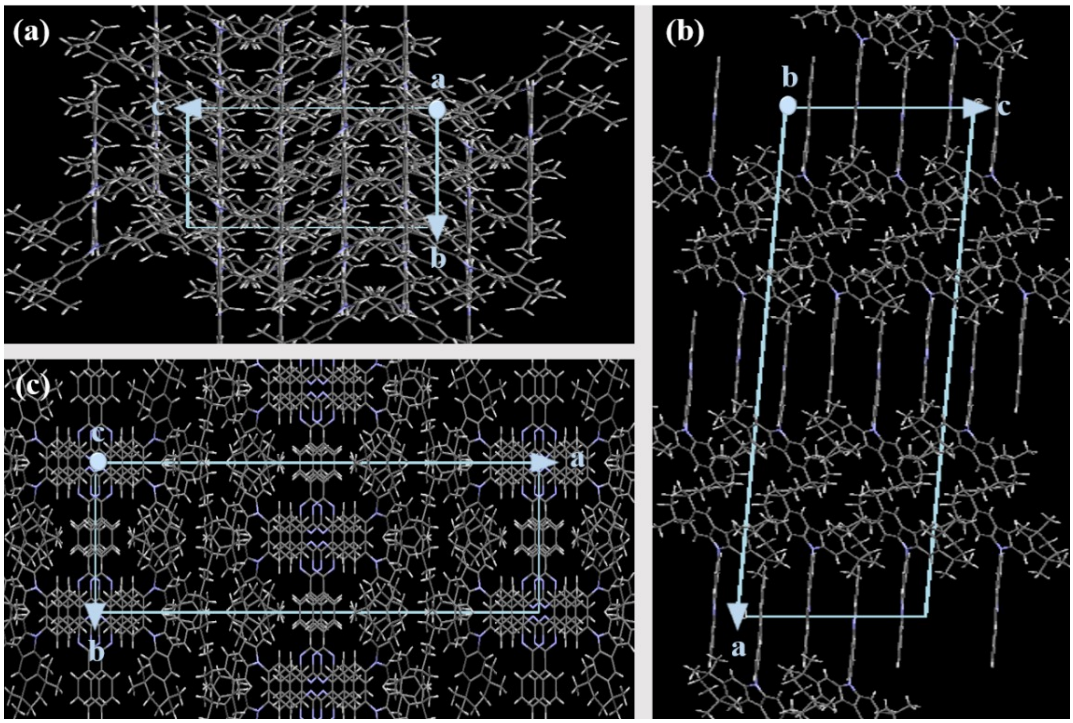


**Figure S8**. Views of molecular packing of Cy2CzTrz from (a) *a* axis, (b) *b* axis and (C) *c* axis, respectively.

**Device part**

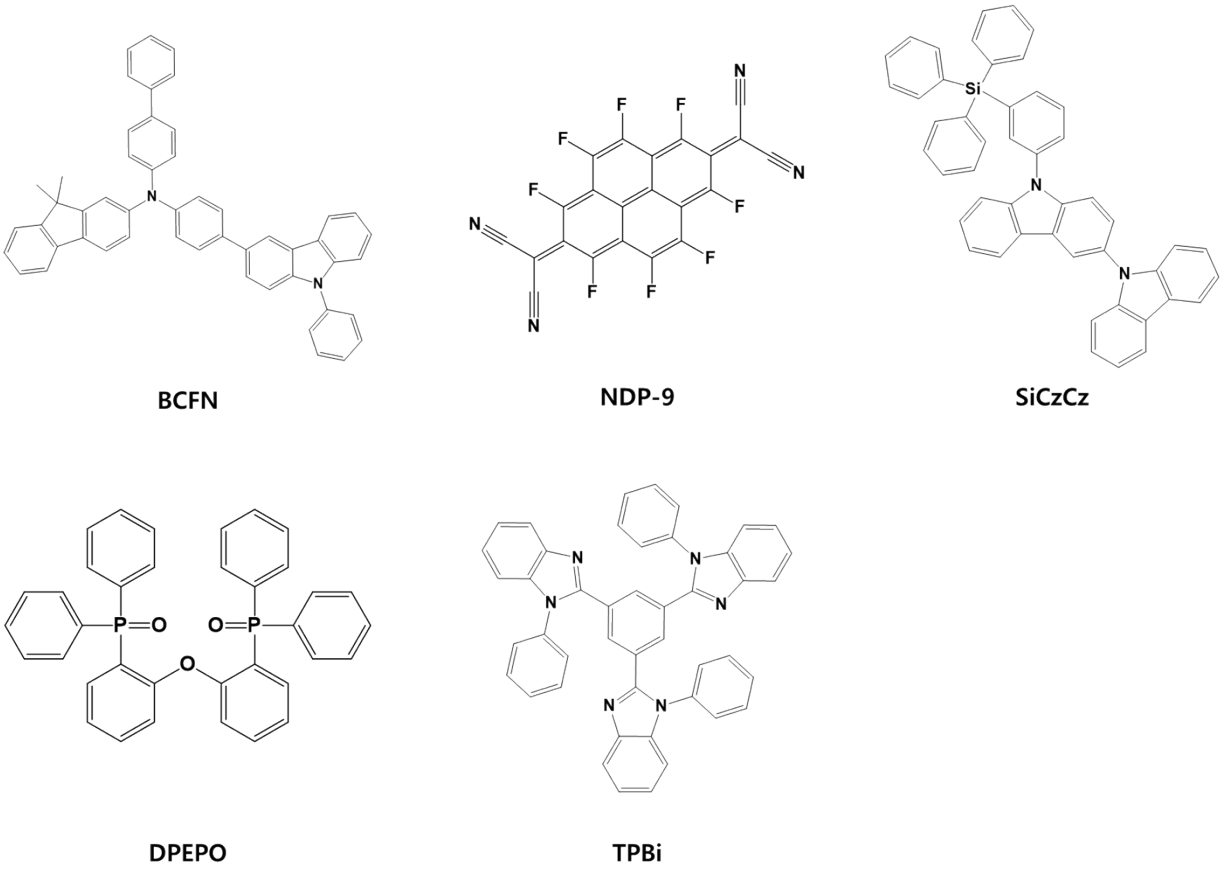


**Figure S9**. The structure of materials used in non-doped devices (D1 and D2).

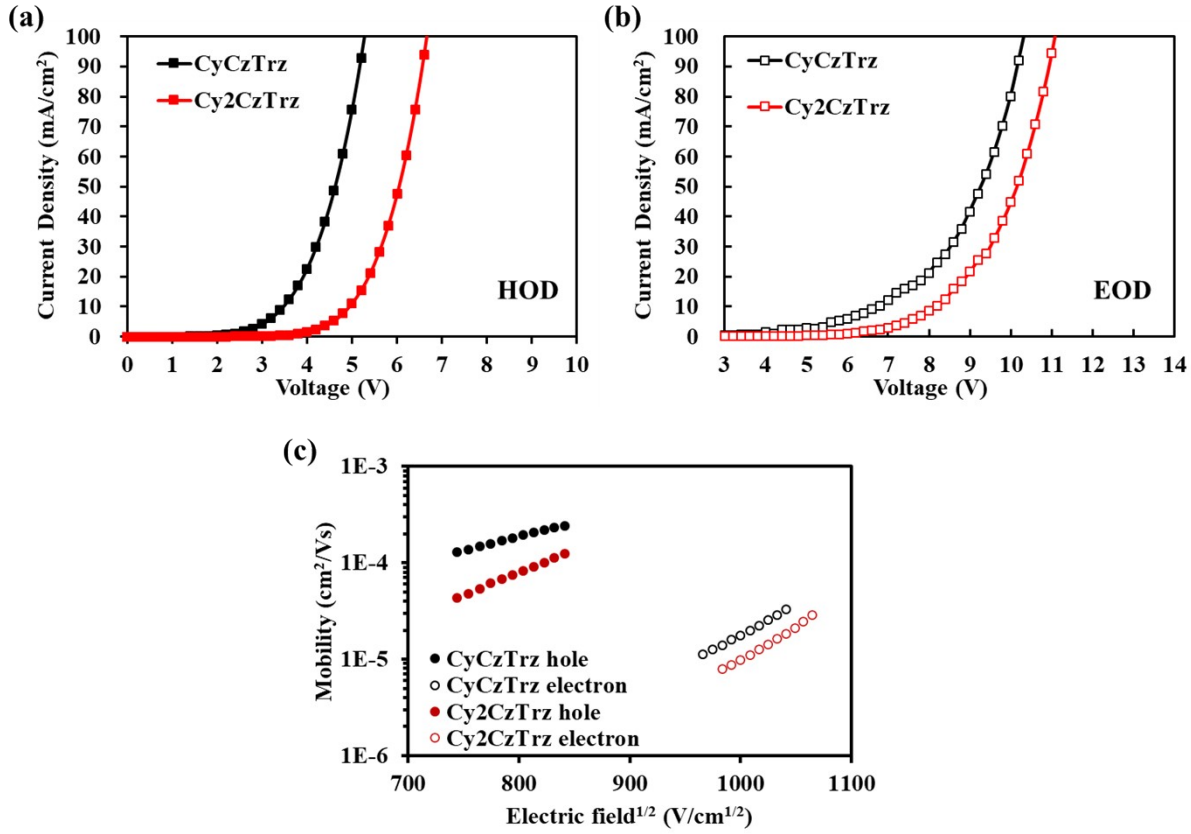


**Figure S10**. (a) Hole only devices (HODs), (b) electron only devices (EODs) of D1 and D2 and (c) the hole and electron mobility of CyCzTrz and Cy2CzTrz calculated form space charge limited current (SCLC) region in HODs and EODs. respectively.

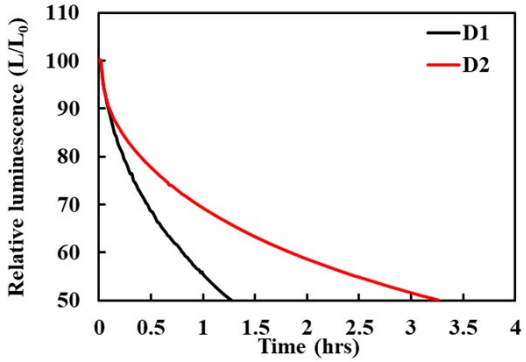


**Figure S11**. The operation lifetime of D1 and D2 measured at 5 mA/cm$^2$.

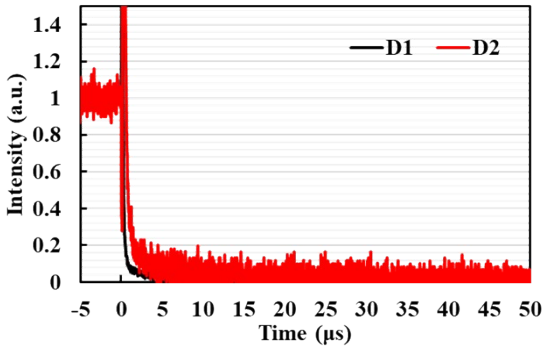


**Figure S12**. The transient electroluminescence (EL) decay of the D1 and D2 measured at 10 mA/cm$^2$.

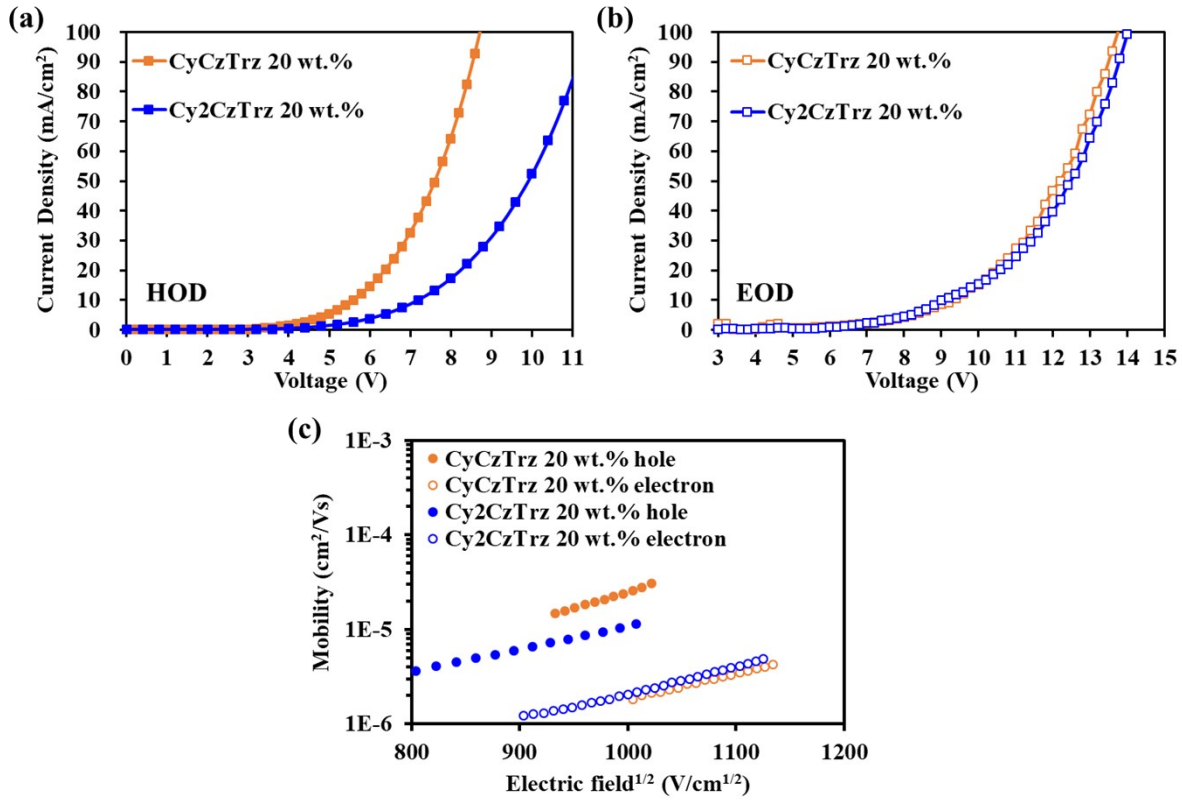


**Figure S13**. (a) HODs and (b) EODs of D1-20 wt.% and D2-20 wt.% and (c) the hole and electron mobility of doped devices calculated form SCLC region in HODs and EODs.

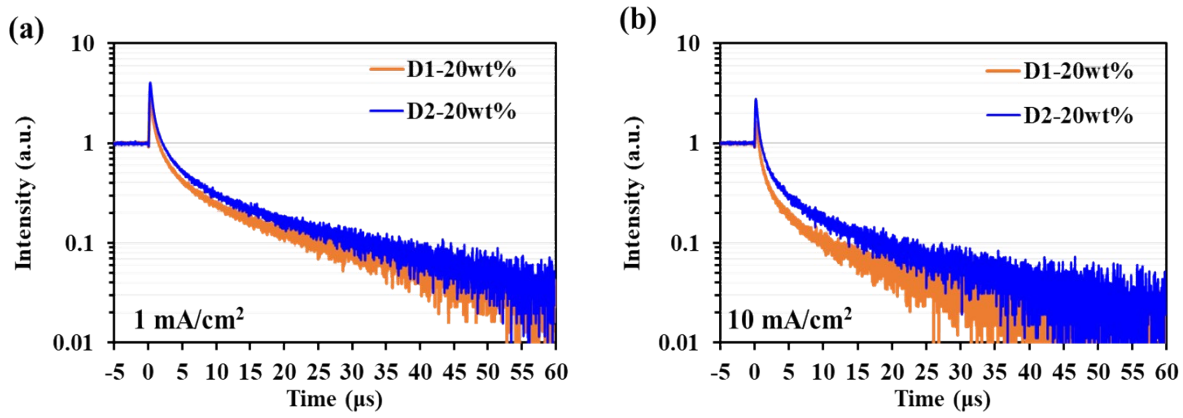


**Figure S14**. The transient EL decay of the D1-20 wt.% and D2-20 wt.% measured at (a) 1 mA/cm$^2$ and (b) 10 mA/cm$^2$.

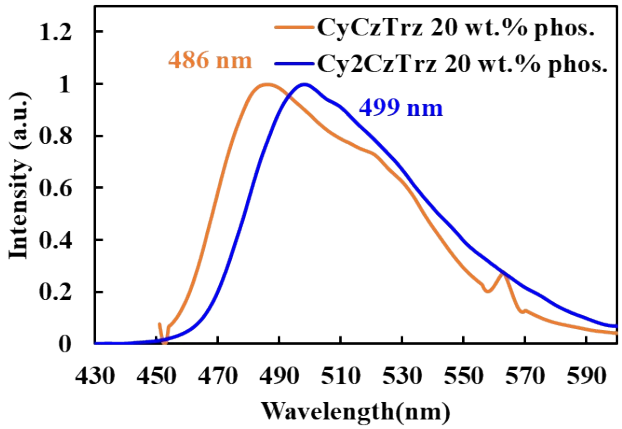


**Figure S15**. The phosphorescence PL spectra of CyCzTrz 20 wt.%: DPEPO and Cy2CzTrz 20 wt.%: DPEPO at 77 K, respectively.

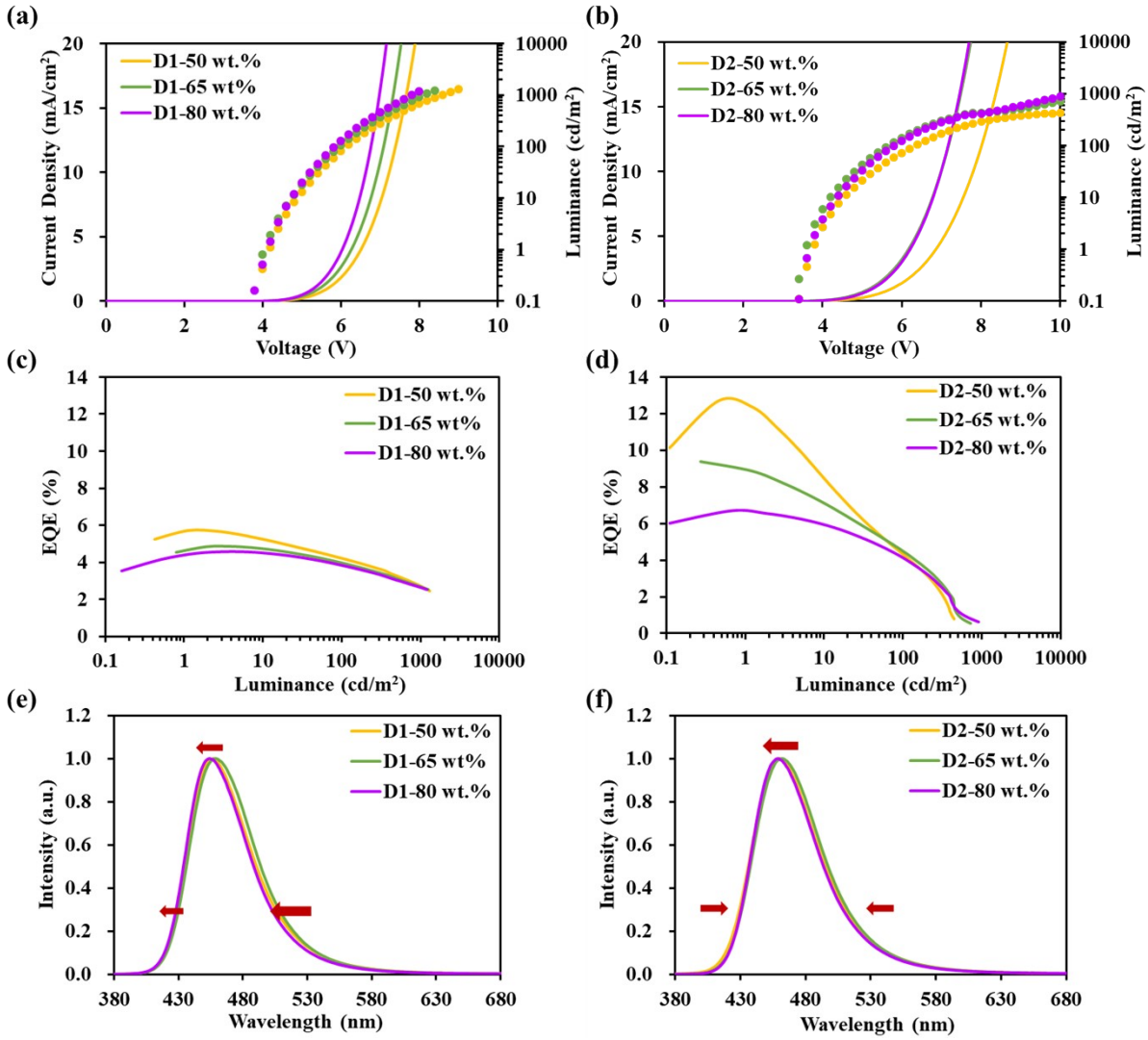


**Figure S16**. (a), (b) The current density(*J*)-voltage(*V*)-Luminance(*L*) curves, (c), (d) EQE curves, and (e), and (f) EL spectra of D1-50 wt.% to 80 wt.% and D2-50 wt.% to 80 wt.% , respectively.

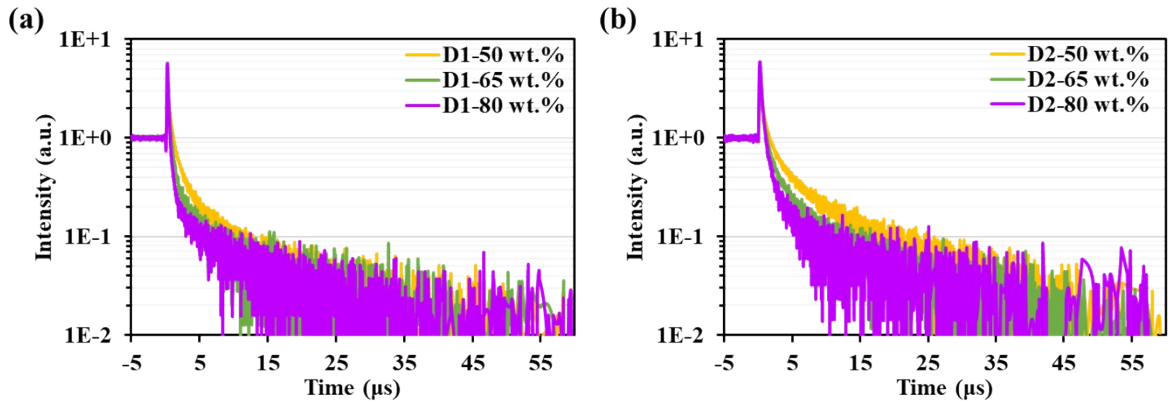


**Figure S17**. The transient EL decay of (a) D1-50 wt.%, 65 wt.% and 80 wt.% and (b) D2-50 wt.%, 65 wt.% and 80 wt.% measured at 10 mA/cm$^2$.

**CyCzTrz**

| Solvents | $\varepsilon$ | $n$ | $f(\varepsilon,n)$ | $\lambda_a$ (nm) | $\lambda_f$ (nm) | $\nu_a$-$\nu_f$ ($cm^{-1}$) |
|---|---|---|---|---|---|---|
| Hexane | 1.89 | 0.08 | 0.001 | 297.1 | 415.0 | 9562.32 |
| Toluene | 2.38 | 1.494 | 0.014 | 298.3 | 435.4 | 10555.9 |
| 1,4-dioxane | 2.21 | 1.422 | 0.021 | 297.6 | 453.8 | 11566 |
| Ethyl acetate | 6.02 | 1.372 | 0.200 | 303.3 | 476.6 | 11988.7 |
| Tetrahydrofuran | 7.58 | 1.407 | 0.210 | 296.7 | 476.2 | 12704.5 |
| Dichloromethane | 8.93 | 1.424 | 0.217 | 297.4 | 498.6 | 13568.6 |
| Dimethyl formamide | 37 | 1.427 | 0.276 | 296.2 | 533.6 | 15020.3 |

**Cy2CzTrz**

| Solvents | $\varepsilon$ | $n$ | $f(\varepsilon,n)$ | $\lambda_a$ (nm) | $\lambda_f$ (nm) | $\nu_a$-$\nu_f$ ($cm^{-1}$) |
|---|---|---|---|---|---|---|
| Hexane | 1.89 | 0.08 | 0.001 | 303.5 | 433.0 | 9853.24 |
| Toluene | 2.38 | 1.494 | 0.014 | 305.6 | 448.0 | 11201.9 |
| 1,4-dioxane | 2.21 | 1.422 | 0.021 | 304.5 | 466.2 | 11390.7 |
| Ethyl acetate | 6.02 | 1.372 | 0.200 | 303.0 | 488.2 | 12519.9 |
| Tetrahydrofuran | 7.58 | 1.407 | 0.210 | 303.0 | 496.6 | 12866.4 |
| Dichloromethane | 8.93 | 1.424 | 0.217 | 304.0 | 530.4 | 14041.0 |
| Dimethyl formamide | 37 | 1.427 | 0.276 | 303.0 | 555.6 | 15004.7 |

**Table S1**. Detailed absorption and emission peak positions of CyCzTrz and Cy2CzTrz in different solvents.

| **Identification code** | CyCzTrz | Cy2CzTrz |
|---|---|---|
| **Empirical formula** | $C_{41}H_{36}N_4$ | $C_{49}H_{50}N_4$ |
| **CCDC number** | 2338676 | 2338677 |
| **Formula weight** | 584.74 g/mol | 694.93 g/mol |
| **Temperature** | 298 K | 298 K |
| **Wavelength** | 1.54184 Å | 1.54184 Å |
| **Crystal system** | Monoclinic | Monoclinic |
| **Space group** | C2/c | C2/c |
| **Unit cell dimensions** | a= 29.4245(2) Å<br>α= 90°<br>b=10.91670(10) Å<br>β= 93.6250(10)°<br>c= 22.6136(2) Å<br>γ= 90° | a= 50.4561(8) Å<br>α= 90°<br>b= 11.4300(2) Å<br>β= 94.074(2)°<br>c= 13.9325(3) Å<br>γ= 90° |
| **Volume** | 7249.37(10) $Å^3$ | 8014.8(3) $Å^3$ |
| **Z** | 8 | 8 |
| **Density (calculated)** | 1.072 $g/cm^3$ | 1.152 $g/cm^3$ |
| **Absorption coefficient** | 0.486 $mm^{-1}$ | 0.512 $mm^{-1}$ |
| **F(000)** | 2480.0 | 2976.0 |
| **Crystal size** | 0.12 x 0.1 x 0.06 mm | 0.18 x 0.16 x 0.05 mm |
| **Theta range for data collection** | 3.010 to 77.847° | 5.047 to 76.767° |
| **Reflections collected** | 59727 | 100688 |
| **Coverage independent reflections** | 100% | 84.5% |
| **Absorption correction** | Multi-scan | Multi-scan |
| **Max. and min. transmission** | 0.971 and 0.944 | 0.975 and 0.913 |
| **Refinement method** | Full-matrix least-squares on $F^2$ | Full-matrix least-squares on $F^2$ |
| **Data / restraints / parameters** | 7685/139/411 | 6995/230/487 |
| **Goodness-of-fit on $F^2$** | 1.064 | 1.023 |
| **Final R indices [I>2sigma(I)]** | I>=2σ(I)<br>$R_1$ = 0.0538,<br>$wR_2$ = 0.1570 | I>=2σ(I)<br>$R_1$ = 0.0819,<br>$wR_2$ = 0.2129 |
| **R indices (all data)** | $R_1$ = 0.0604,<br>$wR_2$ = 0.1623 | $R_1$ = 0.1339,<br>$wR_2$ = 0.2673 |
| **Large diff. peak/hole** | 0.45/-0.43 $eÅ^{-3}$ | 0.30/-0.30 $eÅ^{-3}$ |

**Table S2**. Crystal data and structure refinement for CyCzTrz and Cy2CzTrz.

| Emitter only (30 nm) | V[a)] [V] | $EQE_{max}$ [%] | $\lambda_{max}$[a)] [nm] | CIE (x,y)[b)] | $CE_{max}$ [cd/A] | $PE_{max}$ [lm/W] |
|---|---|---|---|---|---|---|
| **CyCzTrz** | 5.3 | 3.5 | 449 | 0.15, 0.08 | 3.1 | 2.1 |
| **Cy2CzTrz** | 7.2 | 4.9 | 454 | 0.15, 0.11 | 4.9 | 3.7 |

**a) Measured at 10 mA/cm², b) measured at 100 cd/m².**

**Table S3**. Electroluminescence properties of the non-doped devices.

| Compound | $\Delta E_{ST}$ (eV) | $\Phi_{PL}$[a]/$\Phi_{DF}$[b] (%) | $\tau_{PF}$[b] (ns) | $\tau_{DF}$[b] (µs) | $k_{ISC}$ ($10^7$ $s^{-1}$) | $k_{RISC}$ ($10^5$ $s^{-1}$) | $k_{PF}$ ($10^8$ $s^{-1}$) | $k_{DF}$ ($10^4$ $s^{-1}$) | $k_{nr}^S$ ($10^4$ $s^{-1}$) | $k_{nr}^T$ ($10^4$ $s^{-1}$) |
|---|---|---|---|---|---|---|---|---|---|---|
| **CyCzTrz** | 0.18 | 95.6/0.23 | 7.27 | 8.19 | 1.93 | 0.32 | 1.00 | 2.76 | 1.81 | 0.45 |
| **Cy2CzTrz** | 0.15 | 98.8/0.38 | 6.65 | 4.39 | 3.64 | 1.31 | 0.93 | 8.40 | 0.46 | 0.26 |

**a) Absoluted photoluminescence quantum yield measured using an integrating sphere, b) Determined from the integrated area of DF and PF contributions in transient PL.**

**Table S4**. Photophysical parameters of CyCzTrz and Cy2CzTrz in doped films (20 wt% in DPEPO) at room temperature.

| DPEPO : Emitter (30 nm:20 wt.%) | V[a)] [V] | $EQE_{max}$ [%] | $\lambda_{max}$[a)] [nm] | CIE (x,y)[b)] | $CE_{max}$ [cd/A] | $PE_{max}$ [lm/W] |
|---|---|---|---|---|---|---|
| **CyCzTrz** | 7.5 | 7.1 | 462 | 0.14, 0.14 | 8.7 | 6.6 |
| **Cy2CzTrz** | 8.0 | 14.5 | 467 | 0.14, 0.15 | 17.3 | 15.1 |

**a) Measured at 10 mA/cm², b) measured at 100 cd/m².**

**Table S5**. Electroluminescence properties of the 20 wt.% doped devices.

| DPEPO:Emitter (30 nm:X wt.%) | | V[a)] [V] | $EQE_{max}$ [%] | $\lambda_{max}$[a)] [nm] | CIE (x,y)[b)] | $CE_{max}$ [cd/A] | $PE_{max}$ [lm/W] |
|---|---|---|---|---|---|---|---|
| **CyCzTrz** | 50 | 7.2 | 5.7 | 457 | 0.15, 0.12 | 6.9 | 5.1 |
| | 65 | 6.9 | 4.9 | 459 | 0.14, 0.13 | 5.5 | 4.1 |
| | 80 | 6.6 | 4.6 | 454 | 0.15, 0.11 | 4.5 | 3.4 |
| **Cy2CzTrz** | 50 | 7.8 | 12.7 | 460 | 0.15, 0.13 | 14.8 | 12.9 |
| | 65 | 7.0 | 9.4 | 462 | 0.14, 0.14 | 11.3 | 10.5 |
| | 80 | 7.0 | 6.7 | 459 | 0.15, 0.13 | 7.5 | 6.5 |

**a) Measured at 10 mA/cm², b) measured at 100 cd/m².**

**Table S6**. Electroluminescence properties of the devices with high doping concentrations.

| **Emissive layer** | **$V_{on}$ (V)** | **$EQE_{max}$** | **$EL_{max}$ (nm)** | **CIE(x,y)** | **Reference** |
|---|---|---|---|---|---|
| PICzPMO | 3.6 | 19.5 | 506 | (0.227,0.479) | *ACS Appl. Mater. Interfaces*, 2023, **15**, 59643 |
| DPEPO:10%PICzPMO | 3.9 | 20.8 | 487 | (0.210,0.445)) | |
| BCzDPM | 4.9 | 7.05 | 498 | (0.201,0.395) | *J. Lumin.,* 2023, **263**, 120087 |
| ICz-BP | 3.1 | 10.7 | 480 | (0.18, 0.30) | *ACS Appl. Mater. Interfaces*, 2021, **13**, 57713 |
| DPEPO:10%ICz-BP | 3.2 | 17.7 | 475 | (0.17, 0.28) | |
| pCz-BTO | 3.6 | 7.1 | 443 | (0.15, 0.10) | *J. Mater. Chem. C,* 2022, **10**, 3163 |
| DPEPO:10% pCz-BTO | 3.7 | 9.5 | 443 | (0.15, 0.09) | |
| TB-3Cz | | 9.90 | 424 | (0.17, 0.07) | *Adv. Opt. Mater.*, 2020, **8**, 1902175 |
| Mcp:11% *t*Cz-DPPN | 3.6 | 1.7 | 464 | (0.15,0.23) | *J. Mater. Chem. C*, 2024, **12**, 6297 |
| CzAcSF:20% 1TCPM-Cz | 3.8 | 13.3 | 505 | (0.29,0.48) | *Dyes. Pigm.*, 2021, **188**, 109208 |
| mSOAD | 3.1 | 14.0 | 488 | 0.18, 0.32 | *Adv. Opt. Mater.*, 2018, **6**, 1701256 |
| TB-tCz | 3.7 | 8.21 | 416 | (0.17,0.06) | *Adv. Funct. Mater.*, 2021, **31**, 2102588 |
| TB-tPCz | 3.5 | 15.8 | 428 | (0.16,0.05) | |
| TCP-BP-SFAC | 2.7 | 26.1 | 488 | (0.17,0.34) | *Sci. Adv.*, 2021, **7**, eabj2504 |
| DPEPO:25% TCP-BP-SFAC | 3.3 | 38.6 | 480 | (0.16,0.28) | |
| 2Cz2tCzBn | - | 25.8 | 488 @5V | (0.21,0.42)@5V | *J. Mater. Chem. C*, 2020, **8**, 5769 |
| CyCzTrz | 5.3 | 3.5 | 449 | (0.15,0.08) | This work |
| DPEPO:20%CyCzTrz | 7.5 | 7.1 | 462 | (0.14,0.14) | |
| Cy2CzTrz | 7.2 | 4.9 | 454 | (0.15,0.11) | |
| DPEPO:20% Cy2CzTrz | 8.0 | 14.5 | 467 | (0.14,0.15) | |

**Table S7**. Summarized performances of blue devices with CIEy ≤ 0.50 using carbazole based AIE-TADF emitters

## II. Measurements

### *Photophysical, thermal and electrochemical property measurements*

All reactions were performed under a nitrogen atmosphere unless otherwise noted. Reactions were monitored by thin layer chromatography (TLC) using Kieselgel 60 F254 silica gel plates. Flash chromatography was performed over silica gel 60, 230-400 mesh, with the designated solvents. $^{1}$H NMR and $^{13}$C NMR were recorded on a Jeol 500 MHz at room temperature (NMR; JNM-ECZ500R, Jeol Ltd., Tokyo, Japan) serviced by the Center for Bionano Materials Research at Gachon University (Seongnam, Korea). UV-vis absorption spectra were recorded on a UV-1900 spectrometer (Shimadzu). PL spectra were recorded on a Hitachi F-7100 fluorescence spectrophotometer. Differential scanning calorimetry (DSC) was performed on a TA DSC Q2000 at a heating rate of 10 °C min$^{-1}$ under nitrogen. Thermogravimetric analysis (TGA) was performed on a TA SDT 650 instrument at a heating rate of 10 °C min$^{-1}$ under nitrogen. The temperature at 5% weight loss was used as the decomposition temperature ($T_d$). Cyclic voltammetry (CV) was carried out on a WPG100e (WonATech) at room temperature with ferrocenium-ferrocene ($Fc^+/Fc$) as the internal standard. The oxidative scans were performed using 0.1 M n-$Bu_4NPF_6$ ($TBAPF_6$) in deoxygenated dichloromethane as the supporting electrolyte. The cyclic voltammograms were obtained at a scan rate of 0.1 V s$^{-1}$.

## III. OLED fabrication

The indium thin oxide (ITO) coated glass, with a sheet resistance of 30 Ω/sq and a thickness of 150 nm, was cleaned in an ultrasonic bath. Prior to deposition of the organic layer, the -coated glass was dried in a convection oven at 120 ℃ for 10 minutes. Subsequently, the ITO-coated glass underwent O2 plasma treatment for 2 minutes at 2×10-2 Torr and 150 W.

Non-doped device structure: ITO(150 nm)/BCFN:NDP-9 (10 nm, 3 wt.%)/BCFN (60 nm)/ SiCzCz (5 nm)/ CyCzTrz or Cy2CzTrz (30 nm)/ DPEPO (5 nm)/ TPBi (30 nm)/ Liq (1.5 nm)/ Al (100 nm). As the hole injection layer (HIL), 2,2'-(perfluoropyrene-2,7-diylidene)dimalononitrile (NDP-9) doped into N-([1,1'-biphenyl]-4-yl)-9,9-dimethyl-N-(4-(9-phenyl-9H-carbazol-3-yl)phenyl)-9H-fluoren-2-amine (BCFN) with a conventration of 3 wt.%. The hole transporting layer (HTL) solely consisted of BCFN. The electron transporting (ETL) was formed using 1,3,5-tris(1-phenyl-1H-benzo[d]imidazol-2-yl)benzene (TPBi), and 8-Quinolinolato lithium (Liq) was employed as the electron injection layer (EIL). 9-(3-(triphenylsilyl)phenyl)-9H-3,9'-bicarbazole (SiCzCz) was used as the electron blocking layer (EBL), and Bis[2-(diphenylphosphino)phenyl]ether oxide (DPEPO) was employed as the hole blocking layer (HBL). CyCzTrz and Cy2CzTrz were individually utilized as the emissive layer (EML).

Non-doped HOD and EOD device structure, respectively: ITO (150 nm)/ BCFN:NDP-9 (10 nm:3 wt.%)/ BCFN (60 nm)/ SiCzCz (5 nm)/ EML (CyCzTrz or Cy2CzTrz, 30 nm)/ HAT-CN (10 nm)/ Al (100 nm) and ITO (150 nm)/ TPBi (30 nm)/ EML (CyCzTrz or Cy2CzTrz, 30 nm)/ TPBi (30 nm)/ Liq (1.5 nm)/ Al (100 nm).

Doped device structure: The device structure was identical to the non-doped device, featuring EML doped with 20 wt.% of CyCzTrz and Cy2CzTrz in DPEPO., respectively.

Doped HOD and EOD: The structure of HODs and EODs is same as non-doped HODs and EODs, respectively. In the EML, 20 wt.% CyCzTrz and 20 wt.% Cy2CzTrz in DPEPO were fabricated, respectively.

## III. $^{1}$H NMR of CyCzTrz and Cy2CzTrz in $CDCl_3$

**< CyCzTrz >**

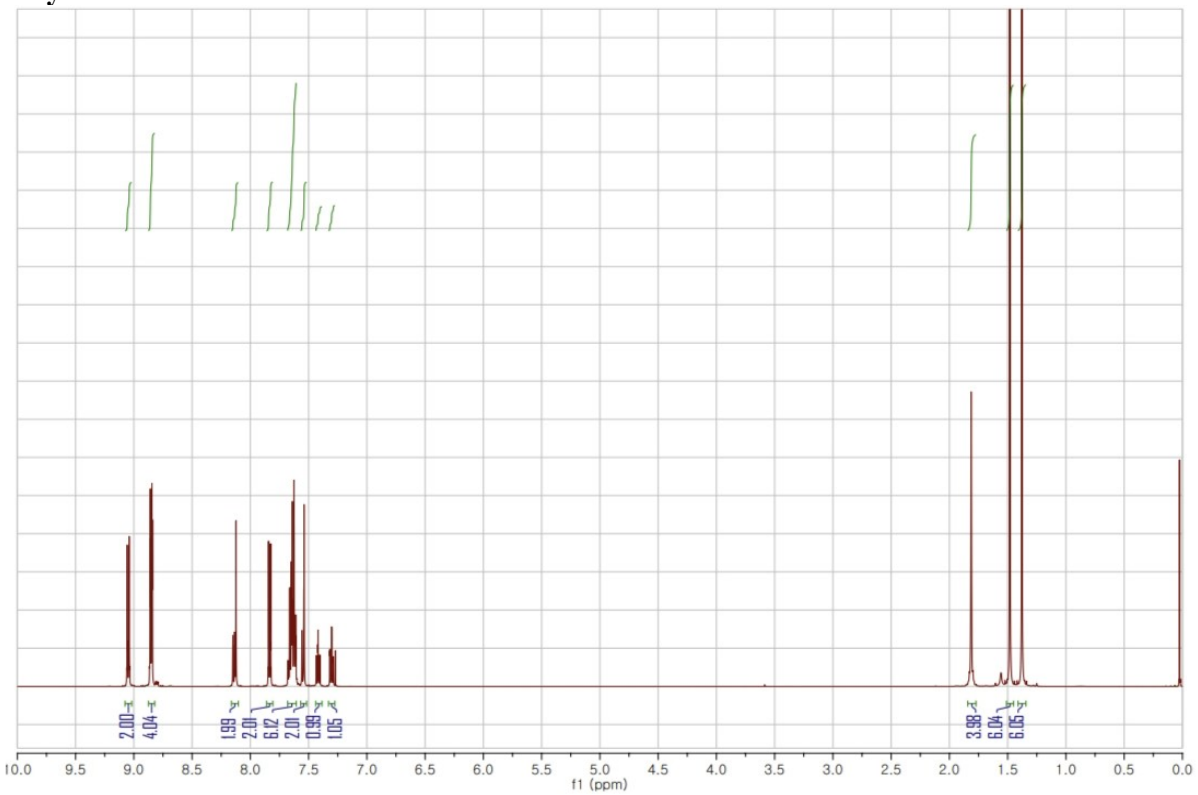


**< Cy2CzTrz >**

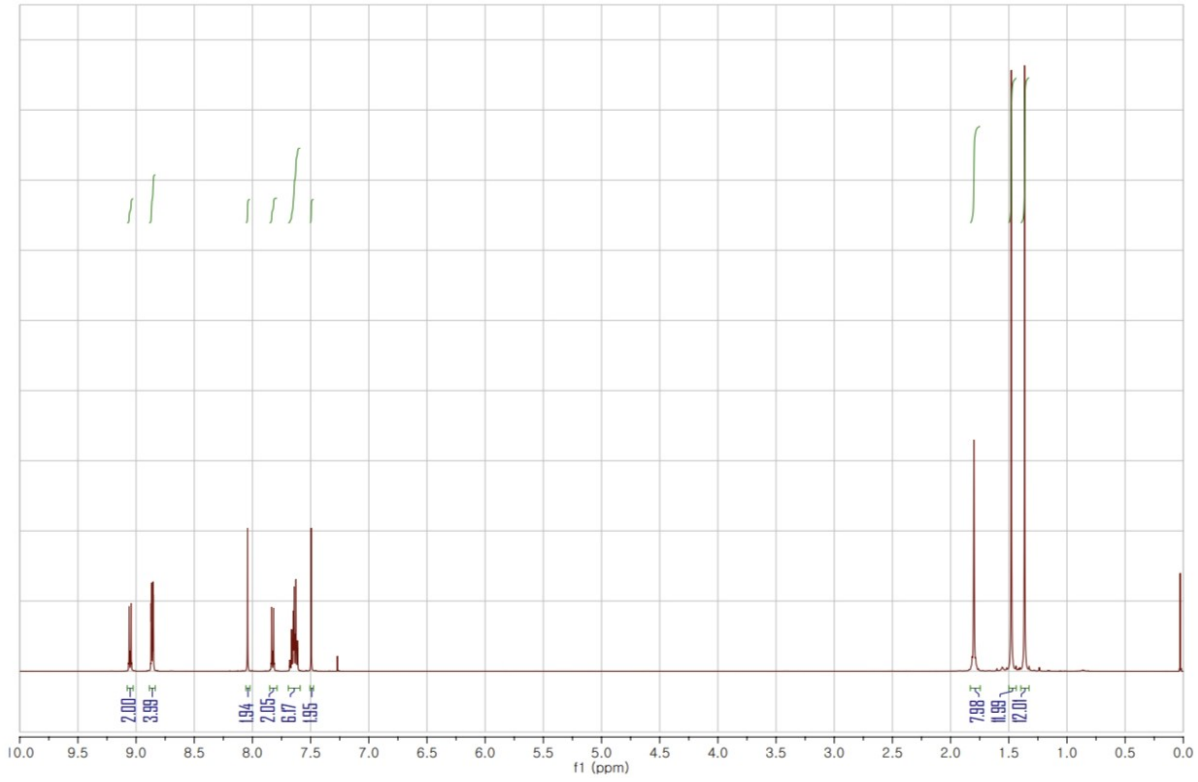

## IV. $^{13}C$ NMR of CyCzTrz and Cy2CzTrz in $CDCl_3$

**< CyCzTrz >**

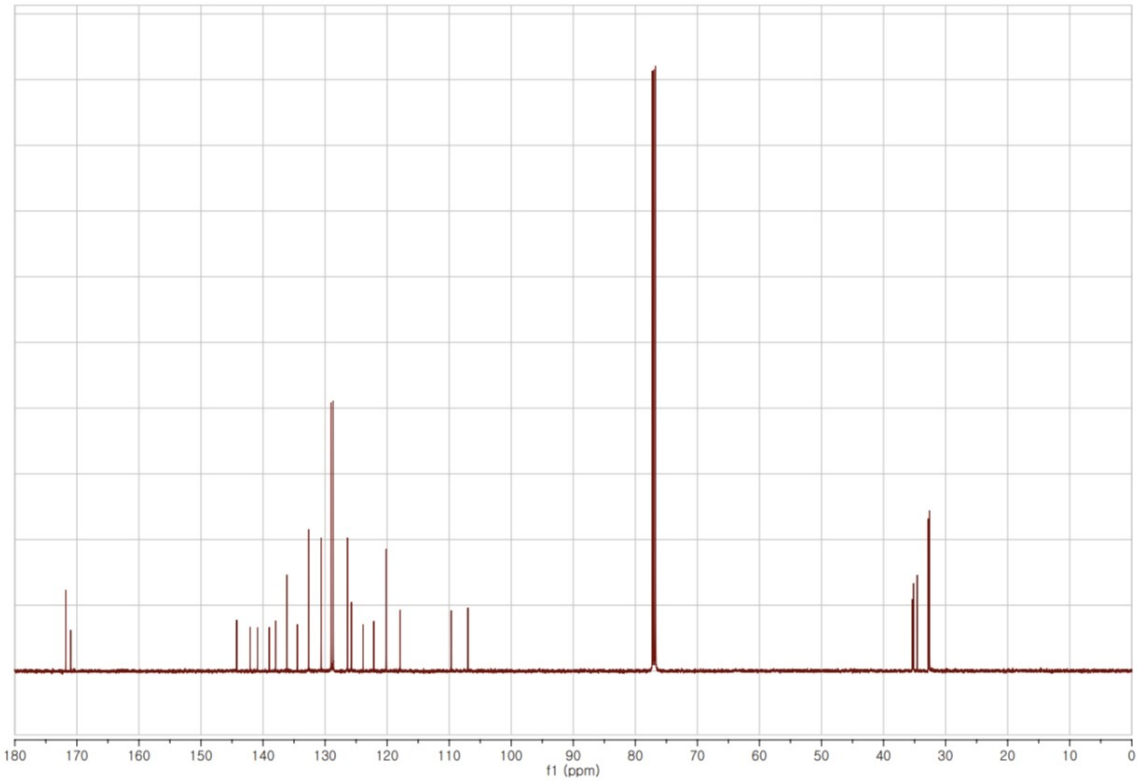


**< Cy2CzTrz >**

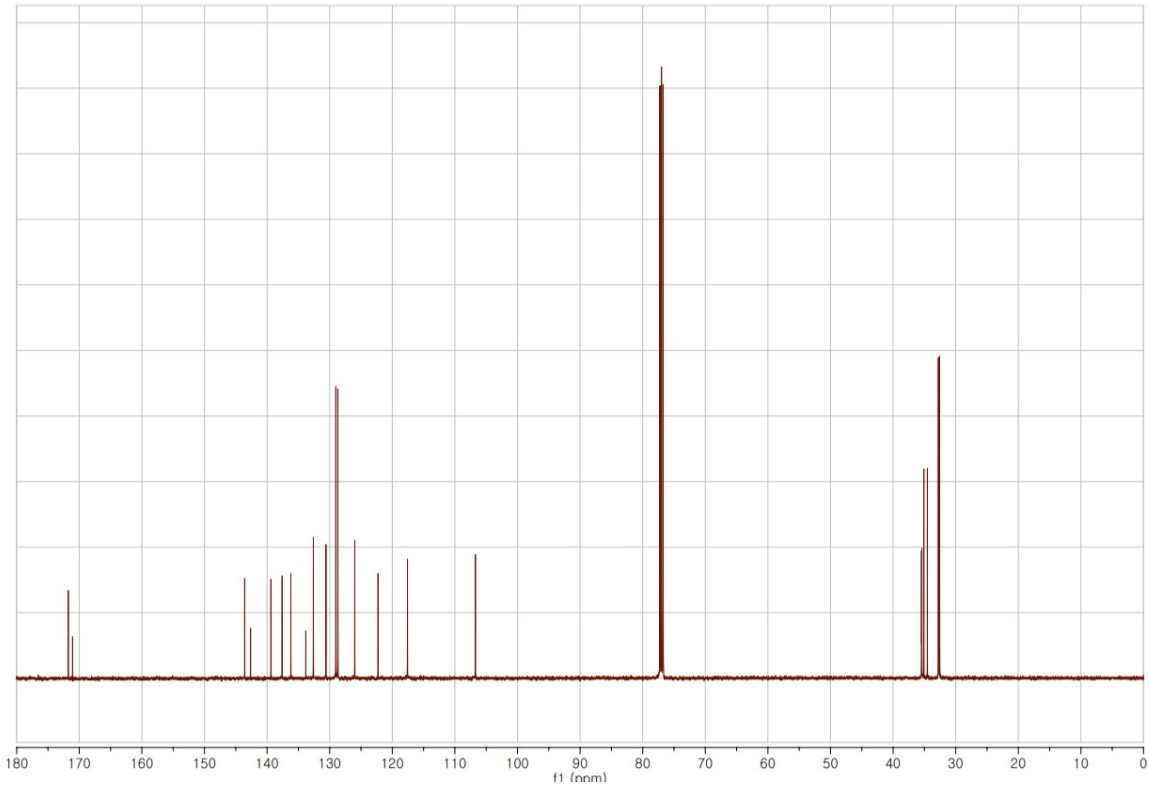

## V. HR-MS of CyCzTrz and Cy2CzTrz

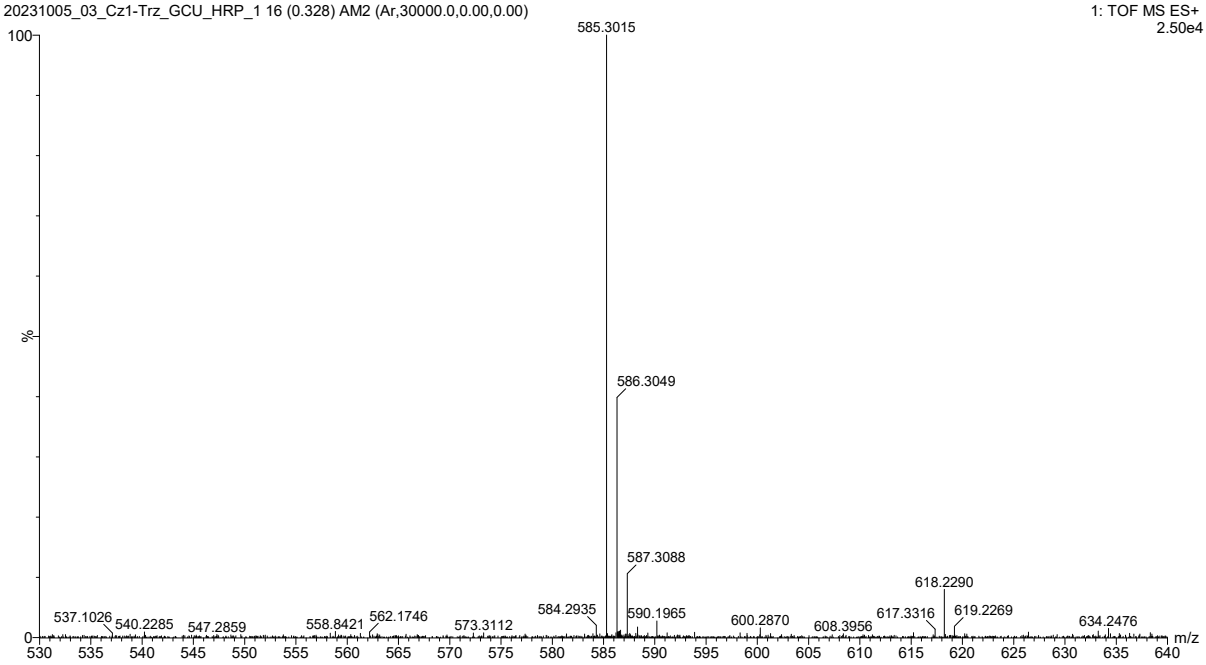


**Elemental Composition Report**

Single Mass Analysis

Tolerance = 5.0 PPM / DBE: min = -1.5, max = 50.0

Element prediction: Off

Number of isotope peaks used for i-FIT = 3

Monoisotopic Mass, Even Electron Ions

70 formula(e) evaluated with 2 results within limits (up to 50 closest results for each mass)

Elements Used:

C: 0-43 H: 0-300 N: 0-5 Na: 0-1

| | | | | | | | | |
|---|---|---|---|---|---|---|---|---|
| Minimum: | | | | -1.5 | | | | |
| Maximum: | | 5.0 | 5.0 | 50.0 | | | | |
| Mass | Calc. Mass | mDa | PPM | DBE | i-FIT | Norm | Conf(%) | Formula |
| 585.3015 | 585.3018 | -0.3 | -0.5 | 25.5 | 433.3 | 0.236 | 78.95 | C41 H37 N4 |

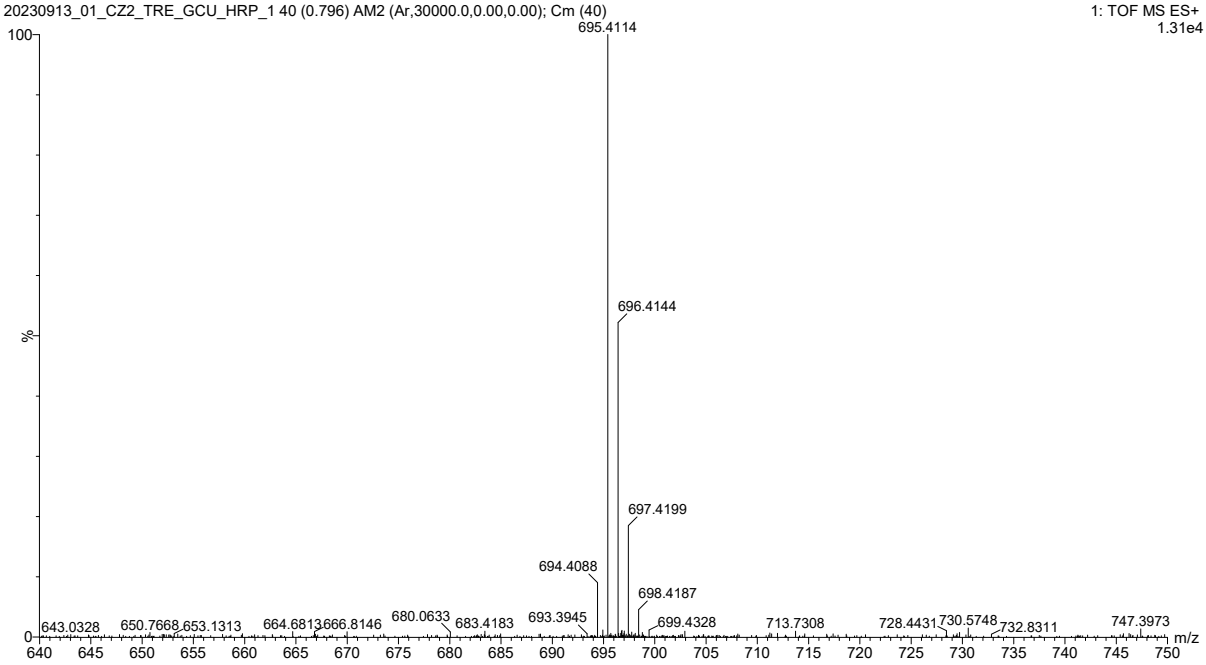


**Elemental Composition Report**

Single Mass Analysis
Tolerance = 5.0 PPM / DBE: min = -1.5, max = 50.0
Element prediction: Off
Number of isotope peaks used for i-FIT = 3

Monoisotopic Mass, Odd and Even Electron Ions
27 formula(e) evaluated with 1 results within limits (up to 50 closest results for each mass)
Elements Used:
C: 0-50 H: 0-300 N: 0-5

| | | | | | | | | |
|---|---|---|---|---|---|---|---|---|
| Minimum: | | | | -1.5 | | | | |
| Maximum: | | 5.0 | 5.0 | 50.0 | | | | |
| Mass | Calc. Mass | mDa | PPM | DBE | i-FIT | Norm | Conf(%) | Formula |
| 695.4114 | 695.4114 | 0.0 | 0.0 | 26.5 | 289.0 | n/a | n/a | C49 H51 N4 |